International Journal of Pharmaceutics 430 (2012) 350–358

Contents lists available at SciVerse ScienceDirect

International Journal of Pharmaceutics

journal homepage: www.elsevier.com/locate/ijpharm

Pharmaceutical nanotechnology

Enhanced antitumor efficacy, biodistribution and penetration of docetaxel-loaded biodegradable nanoparticles

Qin Liu[a], Rutian Li[a], Zhenshu Zhu[b], Xiaoping Qian[a], Wenxian Guan[c], Lixia Yu[a], Mi Yang[a], Xiqun Jiang[d], Baorui Liu[a,*]

[a] The Comprehensive Cancer Center of Drum-Tower Hospital, Medical School of Nanjing University & Clinical Cancer Institute of Nanjing University, Nanjing 210008, PR China
[b] Department of Pharmaceutical Analysis, China Pharmaceutical University, Nanjing 210009, PR China
[c] The Surgery department of Drum-Tower Hospital, Medical School of Nanjing University, Nanjing 210008, PR China
[d] Laboratory of Mesoscopic Chemistry and Department of Polymer Science & Engineering College of Chemistry & Chemical Engineering, Nanjing University, Nanjing 210093, PR China

ARTICLE INFO

Article history:
Received 19 December 2011
Received in revised form 7 March 2012
Accepted 5 April 2012
Available online 12 April 2012

Keywords:
Nanoparticles
Docetaxel
Antitumor
Biodistribution
Tumor penetration

ABSTRACT

To investigate the antitumor effect, biodistribution and penetration in tumors of docetaxel (DOC)-loaded polyethylene glycol–poly(caprolactone) (mPEG–PCL) nanoparticles on hepatic cancer model, DOC-loaded nanoparticles (DOC-NPs) were prepared with synthesized mPEG–PCL by nano-precipitated method with satisfactory encapsulation efficiency, loading capacity and size distribution. The fabricated nano-drugs were effectively transported into tumoral cells through endocytosis and localized around the nuclei in the cytoplasm. In vitro cytotoxicity test showed that DOC-NPs inhibited the murine hepatic carcinoma cell line H22 in a dose-dependent manner, which was similar to Taxotere®, the commercialized formulation of docetaxel. The in vivo biodistribution performed on tumor-bearing mice by NIRF real-time imaging demonstrated that the nanoparticles achieved higher concentration and longer retention in tumors than in non-targeted organs after intravenous injection. The immunohistochemical analysis demonstrated that the nanoparticles located not only near the tumoral vasculatures, but also inside the tumoral interior. Therefore, DOC-NPs could penetrate into tumor parenchyma, leading to high intratumoral concentration of DOC. More importantly, the in vivo anti-tumor evaluation showed that DOC-NPs significantly inhibited tumor growth by tumor volume measurement and positron emission tomography and computed tomography (PET/CT) imaging observation. Taken together, the reported drug delivery system here could shed light on the future targeted therapy against hepatic carcinoma.

© 2012 Elsevier B.V. All rights reserved.

1. Introduction

Hepatocellular carcinoma (HCC) is one of the main leading causes of cancer-related death, especially in Asia, with increasing incidence in developing countries. In contrast to most other malignancies, the systemic chemotherapy is of limited value for HCC (Thomas and Zhu, 2005; Zhu et al., 2010). Insufficient drug uptake and penetration in tumors are the main obstacles for successful treatment. Taxanes, including paclitaxel (PTX) and docetaxel (DOC) are able to disrupt microtubule function, inducing cell apoptosis and death, and have been widely applied for chemotherapy in various cancers. However, the high hydrophobicity of Taxanes influenced their anticancer activity in clinical application (Yan et al., 2010; Cho et al., 2011). And nonspecific toxicities of Taxanes against normal organs resulted in intolerable side effects (e.g., bone marrow depression, hypersensitivity reactions, febrile neutropenia, gastrointestinal tract reaction and skin toxicity) on patients (Baker et al., 2009; Bissery et al., 1995). Recently, there have been a number of carriers which are reported to enhance the delivery and effectiveness of Taxanes. The most striking progress is that intravenous albumin-bound PTX nanoparticles (Abraxane) have been approved for breast cancer treatment in 2005. It was reported that higher intratumoral PTX concentrations and improvement in breast cancer progression-free survival and overall survival were achieved by this formulation (Gradishar et al., 2005). Thus, it is of promising value to develop an intravenously injectable aqueous formation for DOC for hepatoma therapy.

Biodegradable polymer nanoparticles for drug delivery have received considerable attention in cancer targeted therapeutics during the past few decades. In order to prolong the blood circulation and increase tumor accumulation of nanoparticles, the modification of polymer with hydrophilic poly(ethylene glycol) (PEG) has been proposed (Gao et al., 2009; Wu et al., 2009; Zhu, 2010). PEGylation can reduce serum protein adherence and create a stealth surface to prolong the circulating time through avoiding the uptake by the reticuloendothelial systems

* Corresponding author. Tel.: +86 25 83105082; fax: +86 25 83105082.
E-mail address: baoruiliu@nju.edu.cn (B. Liu).

0378-5173/$ – see front matter © 2012 Elsevier B.V. All rights reserved.
http://dx.doi.org/10.1016/j.ijpharm.2012.04.008

(RES). The concentrations of the encapsulated drugs selectively increase in the drug concentration at the tumor sites by enhanced permeability and retention (EPR) effect. On the other hand, efficient extravasation and tumor penetration are important prerequisites for targeting cancer cells (Wong et al., 2011; Cabral et al., 2011). Many drug-encapsulated polymeric nanoparticles are mainly focused on developing DOC formulations that exhibit greater antitumor efficacy and less toxicity than free drug in animal tests. It has been reported that the spread of nanoparticles in tumors is poor because of increased interstitial fluid pressure (IFP) caused by leaky vasculature and poor lymphatic drainage of tumor, resulting in limited therapeutic effect and tumor regeneration. Until now, few studies on the penetration of polymeric nanoparticles in solid tumors in vivo have been reported (Liu et al., 2008a; Wu et al., 2009; Du et al., 2011; Salzano et al., 2011).

In the present study, we prepared DOC loaded PEG-PCL nanoparticles (DOC-NPs) by a modified nanoprecipitation method for intravenous injection. The antitumor efficacy of the nanoparticles was measured by in vitro and in vivo studies. The in vivo real-time near-infrared fluorescence (NIRF) imaging and immunofluorescence staining were also conducted to investigate the performance and penetration of nanoparticles in tumor-bearing mice.

2. Materials and methods

2.1. Materials

DOC was offered by Jiangsu Hengrui Pharmceutical Co. Ltd. (Jiang Su, China). Methoxy-polyethyleneglycol (mPEG) (MW: 4 kDa, Sigma, USA) was dehydrated by azeotropic distillation with toluene, and vacuum dried before use. ε-Caprolactone (ε-CL, Aldrich, USA) was purified by drying over CaH_2 at room temperature and distillation under reduced pressure. Stannous octoate (Sigma, USA) was used as received. All other analytical grade chemicals were used without further purification. Murine hepatic carcinoma cell line H22 was purchased from Shanghai Institute of Cell Biology (Shanghai, China).

2.2. Synthesis of mPEG and PCL block copolymers

mPEG–PCL diblock copolymers were synthesized by a ring open copolymerization as we previously reported (Li et al., 2009). Briefly, predetermined amount of CL and mPEG were added into a polymerization tube containing a small amount of stannous octoate (0.1%, w/w). The tube was sealed off, and placed in an oil bath at 130 °C for 48 h under vacuum condition. Then the crude copolymers were dissolved with dichloromethane (DCM) and precipitated into an excess amount of cold methanol to remove the un-reacted monomer and oligomer. The precipitates were filtered and washed with water several times before dried.

2.3. Preparation of DOC-loaded mPEG–PCL nanoparticles

DOC-loaded mPEG–PCL nanoparticles were prepared by a nanoprecipitated method. Briefly, 10 mg mPEG–PCL block copolymers and 5 mg DOC were dissolved in hot acetone and added dropwise into 50 °C distilled water. The remaining acetone was removed by vacuum evaporation at room temperature. The resulted bluish aqueous solution was filtered through a 0.22 μm filter membrane to remove non-incorporated drugs and copolymer aggregates. Empty nanoparticles were prepared in a similar manner in the absence of DOC. The prepared nanoparticles were lyophilized for further use.

2.4. Drug loading content and encapsulation efficiency of DOC-NPs

The drug loading content and encapsulation efficiency of DOC-NPs were analyzed by a High Performance Liquid Chromatography (HPLC) system with a HC-C18 analytical column (250 mm × 4.6 mm, 5 μm, C18, Agilent Technologies, Palo Alto, USA). The mobile phase consisted of acetonitrile (HPLC grade, Merck)/double-distilled water (Millipore, Milford, USA) (50/50, v/v) with 1.0 mL/min flow rate at 35 °C. The retention time of DOC was at about 3.4 min with 230 nm UV detection wavelength. The drug loading content and encapsulation efficiency were calculated by Eqs. (1) and (2), respectively.

$$\text{Drug loading content}\,(\%) = \frac{\text{Weight of the drug in nanoparticles}}{\text{Weight of the nanoparticles}} \times 100 \quad (1)$$

$$\text{Encapsulation efficiency}\,(\%) = \frac{\text{Weight of the drug in nanoparticles}}{\text{Weight of the feeding drug}} \times 100 \quad (2)$$

2.5. Size and morphology of the nanoparticles

The morphology of the nanoparticles was determined on the transmission electron microscopy (TEM, JEM-100 S, JEOL, Japan). The sample was negative stained with 1% (w/v) phosphotungstic sodium solution and placed on a copper grid covered with nitrocellulose membrane. Scanning electron microscopy (SEM) (S-4800, HITACHI, Japan) was also conducted to characterize the nanoparticles. One drop of nanoparticles suspension was placed on a clean silicon wafer and air-dried at room temperature before observation.

2.6. In vitro DOC release from the nanoparticles

25 mg lyophilized DOC-loaded nanoparticles were redispersed in 1 mL of phosphate buffer solution (PBS, 0.01 M, pH 7.4) and put into a dialysis bag (MWCO: 12 kDa). The dialysis bag was immerged into 5 mL human plasma with gentle agitation at 37 °C for 96 h. At different time points, the release medium was withdrawn for HPLC analysis, and equivalent release medium was added.

2.7. In vitro cellular uptake

For the cellular uptake studies, the particles were firstly labeled with Rhodamine B isothiocyanate through the reaction between isothiocyanate and hydroxyl end group of PCL block. Briefly, Rhodamine B isothiocyanate and mPEG–PCL copolymers were dissolved in DMF for reaction 10 h. Afterwards, the unconjugated Rhodamine B isothiocyanate was removed by dialysis against deionized water for 48 h (MWCO: 10 kDa). The insoluble fluorescent dye coumarin-6 was used as a probe to imitate DOC. In brief, the coumarin-6 was added to the polymer solution in acetone. Then the dye–polymer solution was added to the deionized water quickly to form the nanoparticles. The remained acetone was removed by vacuum. 10^5 H22 cells were plated in a 6-well plate with RPMI 1640 supplemented with 10% fetal blood serum at 37 °C and 500 μL medium containing coumarin-6 loaded mPEG–PCL nanoparticles (equaled to 6.25 μg/mL coumarin-6 in medium) was added for incubation 1 and 4 h at 37 °C. The cells were collected and washed three times with PBS. Then the cells were resuspended in serum-free media and observed under a laser scanning confocal microscopy (Zeiss, LSM510, Germany).

2.8. In vitro cytotoxicity of DOC-loaded nanoparticles

Cytotoxicity of DOC-loaded nanoparticles against murine hepatic carcinoma cell line H22 was assessed by 3-(4,5-dimethylthiazol-2-yl)-2,5-diphenyltetrazolium (MTT) assay.

Briefly, cells were seeded in 96 well plates (8000/well) in RPMI 1640 with 10% fetal bovine serum at 37 °C with 5% CO_2. After 24 h, the cells were cultured with various concentrations of Taxotere® and DOC-NPs for 48 h. Then 20 μL MTT solution (5 mg/mL) was added to each well and incubated for 4 h in dark. The medium was removed and 150 μL dimethyl sulfoxide (DMSO) were added to each well to dissolve the dark-blue formazan crystals. The absorption of each well at test and reference wavelengths of 490 nm and 630 nm was measured by an ELISA reader (Huadong, DG-5031, Nanjing). Cell viability was determined by the following formula:

$$\text{Cell viability}\,(\%) = \frac{\text{Abs(sample)}}{\text{Abs(control)}} \times 100$$

All the results were obtained by three independent experiments and testing in triplicate each time.

2.9. The real-time biodistribution of nanoparticles in tumor-bearing mice

The real-time biodistribution of mPEG–PCL nanoparticles was investigated by the non-invasive near-infrared fluorescent (NIRF) imaging. NIR-797-isothiocyanate was labeled on the mPEG–PCL nanoparticles to track the position of particles. Briefly, the NIR-797-isothiocyanate and mPEG–PCL copolymers were dissolved in DMF and stirred at room temperature for 8 h. Then unconjugated NIR-797-isothiocyanate was removed by dialysis (MWCO 3500 Da) for 2 days. The NIR-797 labeled nanoparticles solution was lyophilized for further use.

NIR-797 labeled nanoparticles (equivalent to the dose DOC 10 mg/kg in antitumor study) were intravenously administrated into H22 tumor-bearing mice. The real-time biodistribution of nanoparticles in tumor bearing mice was imaged using the IVIS® Lumina system (Xenogen Co., Alameda, CA, USA) at 1 h, 2 h, 4 h, 24 h and 48 h post i.v. administration. The NIRF at 745 nm was collected and exposure time was set to 2 s.

2.10. The penetration of mPEG–PCL nanoparticles in tumor tissues

To investigate the location of mPEG–PCL nanoparticles in the tumor tissues relative to the tumor vasculature, the FITC-labeled mPEG–PCL nanoparticles were injected to H22 tumor-bearing mice. Briefly, 30 mg mPEG–PCL copolymer and 2 mg FITC were dissolved in 1.5 mL DMF, and then the reaction solution was stirred at 32 °C for 12 h. Then the resulted solution was dialysis in 12 kDa for 48 h to remove unreacted FITC. The H22 tumor-bearing mice were injected with FITC labeled nanoparticles (equated to the amount of 10 mg/kg DOC-NPs) and saline. The tumor bearing mice were sacrificed at 6 h and 24 h post administration. For staining of tissue sections, frozen sections (10 μm) were immunostained with polyclonal antibody against CD31. Alexa 594-conjugated anti-donkey antibody was used as secondary antibody (Molecular Probes). The samples were observed under a Zeiss LSM510 Meta confocal microscope for immunohistochemistry.

2.11. In vivo antitumor effect of DOC-loaded nanoparticles

All animal experiments were performed in full compliance with guidelines in the Guide for the Care and Use of Laboratory Animals published by the US National Institutes of Health (NIH publication No. 85-23, revised 1985) and was approved by the Ethics Review Board for Animal Studies of Drum Tower Hospital, Medical School of Nanjing University. ICR mice (5–6 weeks, male, 18–22 g), raised under specific pathogen-free (SPF) were subcutaneously injected at the lower right axilla with 0.1 mL of cell suspension containing 10^7 H22 hepatic cancer cells. The mice whose tumor reached about 100 mm^3 were randomly divided into four groups with each group containing 6 mice and the day was designated as "Day 1", On Day 1, the mice were treated i.v. with saline, empty nanoparticles, commercial Taxotere® (10 mg/kg) and DOC-NPs (10 mg/kg eq.).

Tumor size was measured every other day during the study. The tumor volume was calculated by the formula $W \times L^2/2$, where W is the widest diameter and L is the longest diameter.

2.12. In vivo PET/CT imaging

On the 7th day after DOC administration, mice that received saline, Taxotere® and DOC-NPs were taken randomly for deoxy-2-[^{18}F]fluoro-D-glucose (^{18}FDG) positron emission tomography/computed tomography (PET/CT) imaging to evaluate the early antitumor efficacy. After fasting for 8 h and anesthesia with pentobarbital sodium (40 mg/kg), 100 μCi/0.3 mL fluorin-18-2-fluoro-2-deoxy-D-glucose (^{18}F-FDG) was intravenously injected into the H22 bearing mice. The imaging was performed with a combined PET/CT scanner (Jemini JXL, Philips, USA) for clinical use. PET and CT images were acquired in the prone position 30 min after injection administration of ^{18}F-FDG. The fusion images were collected by the automatic image fusion software. The standard uptake values (SUVs) in the tumors were calculated according to the following formula:

$$\text{SUVs} = \frac{\text{Radioactivity in tumors}\,(\mu\text{Ci/cc})}{\text{Total injected dose}\,(\mu\text{Ci/cc}) \times \text{animal weight}\,(\text{g})}$$

2.13. Statistical analysis

Statistical analyses of data were made by Student's t-test and the data are listed as mean ± SD. Value of $P < 0.05$ was considered statistically significant.

3. Results

3.1. Preparation of DOC-NPs

The mPEG–PCL nanoparticles were synthesized by an open-ring polymerization of ε-caprolactone and mPEG in the present of stannous octoate as we previously reported. The feeding ratio of ε-caprolactone monomer and mPEG were 5:1, which was the most suitable to load drugs according our previous reports (mPEG4k–PCL20k) (Li et al., 2009). The number–average molecular weight and weight–average molecular weight of the samples were 18119.4 Da and 24301.6 Da, respectively. The polydispersity of the mPEG4k–PCL20k copolymer (defined as the ratio of weight–average molecular weight to the number–average molecular weight) was narrow with all 1.34. Fig. 1 shows the morphology images of the nanoparticles obtained from TEM and SEM. All the nanoparticles have a small size (about 70 nm) and a nearly spherical shape with a smooth surface. The insoluble DOC was encapsulated into nanoparticles by a modified nano-precipitated method, with a high drug loading content (about 20%) and encapsulation efficiency (more than 80%).

3.2. In vitro DOC release from DOC-NPs

The in vitro release kinetic of DOC from PEG-PCL nanoparticles was investigated in human plasma to imitate the particles' action in human body. The release of DOC from the nanoparticles had a burst release, with nearly 30.5% drug released from the carriers in

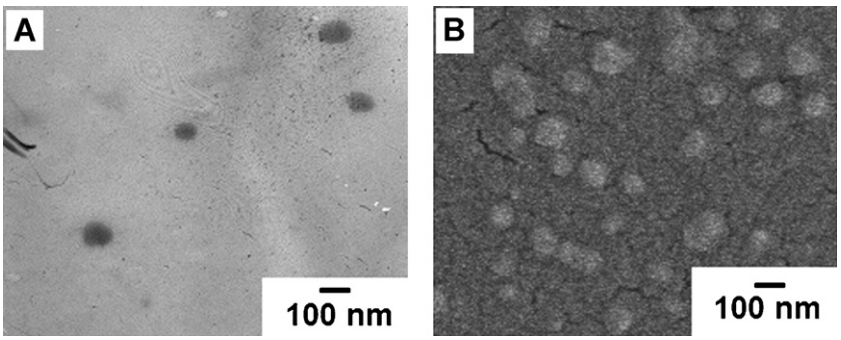

Fig. 1. TEM (A) and SEM (B) images of DOC-NPs: (A) TEM image showed that DOC-NPs were less than 100 nm in size and were in a spherical shape with a smooth surface. (B) SEM image of DOC-NPs confirmed the results obtained from TEM image.

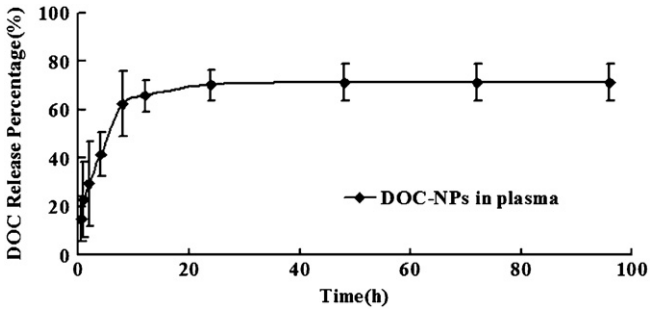

Fig. 2. In vitro DOC release from DOC-loaded nanoparticles in human plasma. The amount of released free and loaded DOC was determined by HPLC as described in Section 2 part.

the first 4 h and about 65% in the first 12 h. After that, a steady sustained release was observed up to 96 h (Fig. 2).

3.3. In vitro cellular uptake

The Rhodamine B isothiocyanate marked fluorescent nanoparticles were applied to study the cellular uptake. In-soluble dye coumarin-6 were encapsulated into nanoparticles to track the position of DOC. We found the fluorescence of coumarin-6 (green) and Rhodamine B (red) was overlapped in the cytoplasm (Fig. 3), and the density of fluorescent signals were increased as time went on, suggesting more and more nanoparticles entered cells. As coumarin-6 was originally entrapped in the nanoparticles, which indicated the drug molecules could effectively penetrate cell membrane barriers and distribute in cell cytoplasm via nanoparticles forms.

3.4. In vitro cytotoxicity of DOC-NPs

To compare the cytotoxicity of the free and encapsulated Taxotere®, H22 cells were exposed to empty PEG-PCL nanoparticles, equivalent concentrations of Taxotere® or DOC-NPs for 48 h, and the percentage of viable cells was quantified using MTT method, which was generally used in cytotoxicity test. We found that empty nanoparticles nearly did not suppress H22 cell proliferation when its concentration reached up to 20 μg/mL, indicating the copolymers were nontoxic to tissues and cells. The cell suppression of Taxotere® and DOC-NPs against H22 cell lines exhibited a dose-depended effect. 46.12% and 44.99% H22 cells are viable when treated with Taxotere® and DOC-NPs at the concentration of 200 ng/mL, respectively (Fig. 4). The similar cytotoxicity between Taxotere® and DOC-NPs against H22 cell lines indicated DOC still kept its pharmacological activity when encapsulated into nanoparticles.

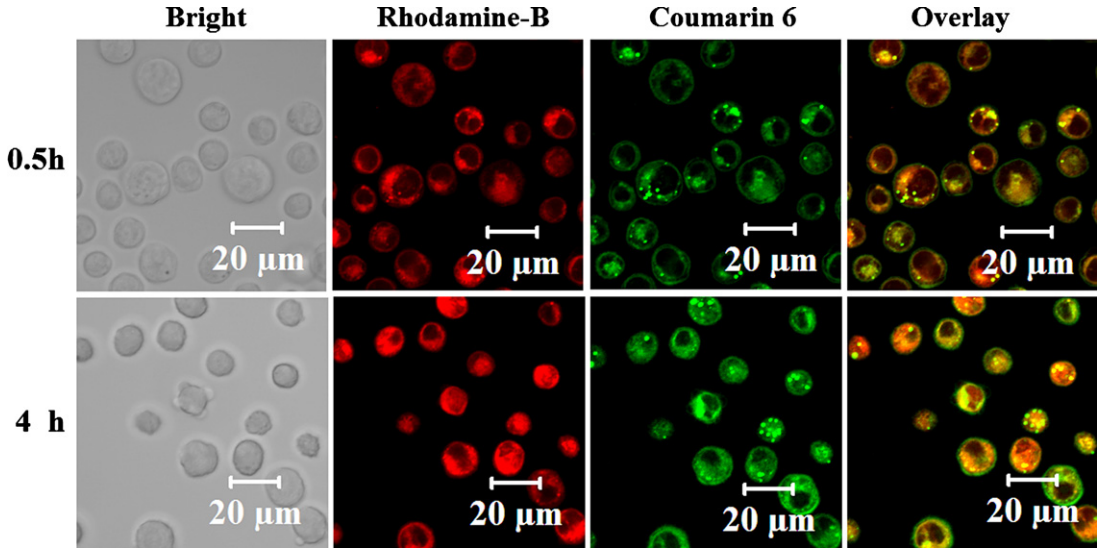

Fig. 3. In vitro H22 cellular uptake studies of nanoparticles. Confocal microscopy images of H22 cells after incubation with coumarin-6-loaded Rhodamine-B labeled mPEG–PCL nanoparticles.

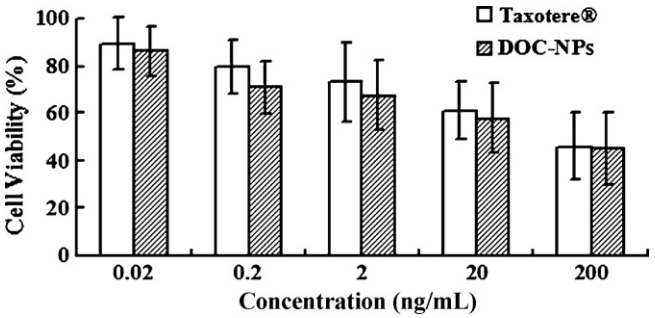

Fig. 4. Cytotoxicity of Taxotere® and DOC-NPs against murine heptacellular carcinoma cells H22 after 48 h incubation. The cytotoxicity of the nanoparticles was determined by the viabilities of cells. The values were represented as mean ± SD ($n = 3$).

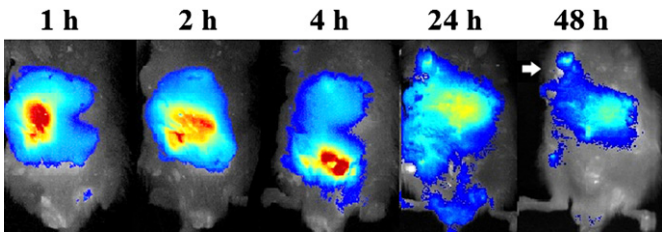

Fig. 5. In vivo NIRF images of H22 tumor-bearing mice following intravenous administration of NIR-797 labeled DOC-NPs during 48 h. The tumors were marked by arrows.

3.5. In vivo imaging of NIR-797 labeled DOC-NPs

To visualize the real-time biodistribution of DOC-loaded nanoparticles in H22 tumor bearing mice, we marked the mPEG–PCL nanoparticles with a NIRF dye (NIR-797) for near-infrared fluorescence imaging. Fig. 5 depicts the NIR fluorescence signals were observed on both tumors and abdomen post 4 h administration. During the first 24 h observation, the fluorescence density of the abdomen decreased, meanwhile NIRF signals gradually increased in tumor. Then the strong fluorescence signal could only be observed in the tumor region at 48 h post administration, which favored the enhanced antitumor efficacy of DOC. At the meantime, the nanoparticles that are not located in tumor zones are able to easily clear from liver and other tissues, implying minimal side effects caused by drugs.

3.6. Penetration of DOC-NPs in tumors

The nano-size PEGylated micelles accumulate and retain at the tumors due to the EPR effect. However, the delivery of drugs to solid tumor cells is easily hindered by high intratumoral fluid pressure. Thus, exploration of real-time tumor targeting distribution and penetration of the nanoparticles is desirable for understanding the effectiveness of tumor chemotherapy.

Particles labeled with fluorescent dyes were frequently used to study their in vivo tumor distribution (Liu et al., 2012; Sugahara et al., 2010; Zhu et al., 2011). We administrated FITC-labeled mPEG–PCL nanoparticles by intravenous injection to confirm the micelles position in the tumor tissues (Fig. 6), whereas the tumor vessels were stained by anti-CD31 antibody. The locations of FITC-labeled NPs (green fluorescence) were observed to be located or around the area stained with the tumor vasculatures (red fluorescence) at 4 h post injection. After 24 h intravenous injection, most nanoparticles still remained in the vascular lumen, but a portion of nanoparticles could been observed about 50 μm away from the blood vessels, demonstrating that the DOC-loaded NPs had the ability to penetrate further away from the blood vessels and interact with more viable cancer cells as time went on.

3.7. In vivo anticancer effect of DOC-NPs

The antitumor effect of DOC-NPs compared with Taxotere® was carried on hepatic H22 transplanted solid tumor bearing mice. Fig. 7

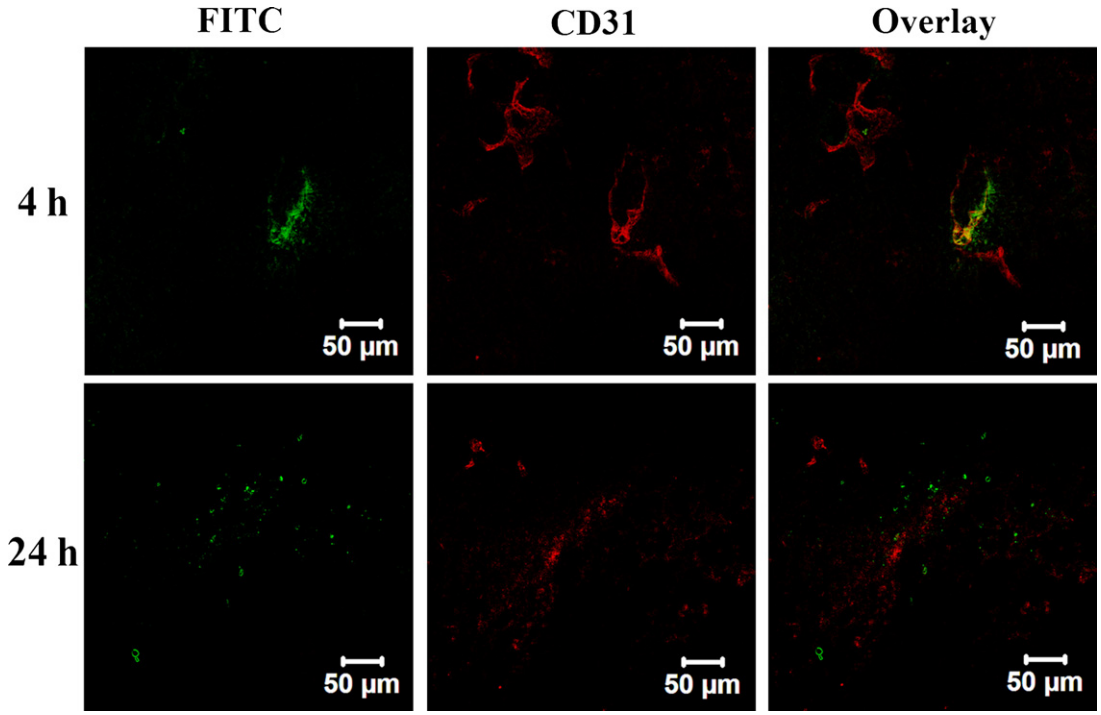

Fig. 6. Penetration of FITC-labeled DOC-NPs in tumor ehanced the antitumor efficacy of docetaxel-loaded biodegradable nanoparticles 4 h (Up) and 24 h (Down) post-injection. CD31 (blood vessels, red) and FITC-labeled nanoparticles (green) costaining images of H22 tumor sections were demonstrated. (For interpretation of the references to color in this figure caption, the reader is referred to the web version of the article.)

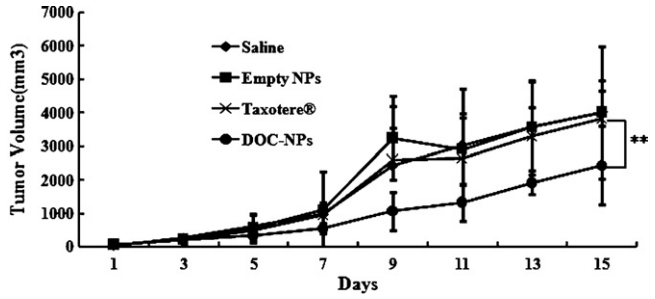

Fig. 7. In vivo tumor growth curves of H22 tumor-bearing mice that received different treatments. The same DOC dose (10 mg/kg) was given by intravenous injection on day 1. Data are presented as mean ± SD ($n = 6$), $^{**}P < 0.01$.

shows the tumor volume variation of the H22 tumor bearing mice received saline, empty NPs, Taxotere® (10 mg/kg) and DOC-NPs (10 mg/kg DOC eq.). The commercial Taxotere® did not inhibit the tumors growth, while DOC-NPs could significantly suppress the fast-growing H22 tumors ($P < 0.01$).

3.8. Intravital PET/CT imaging

The early antitumor effects of saline, Taxotere® and DOC-NPs on tumor activity were evaluated by PET/CT. Fig. 8 reveals the FDG uptake of tumor-bearing mice in saline, Taxotere® and DOC-NPs groups on the 7th day after treatment. The white arrows indicated the location of tumors at the lower right axilla. PET and CT scanning images clearly revealed invisible tumor metabolic activity and tumor size in each group, respectively. The mice treated with saline demonstrated the highest signal intensity, On the contrary, the tumors in the mice receiving DOC-NPs showed the lowest FDG uptake, which signified the lowest tumor metabolism. The quantitative FDG uptake results of each group in tumors were calculated by average standard uptake values (SUVs), which provided a quantitative measure of tissue FDG accumulation. The mean SUVs of tumors in the mice receiving saline, Taxotere® and DOC-NPs were 1.15 ± 0.09, 0.85 ± 0.03, 0.42 ± 0.06, respectively. As the CT imaging displayed, the tumor volume of saline and Taxotere® treated mice were about 1000 mm^3 and 900 mm^3, while the tumor in DOC-NPs treated groups was much smaller than that of other groups.

4. Discussions

Biocompatible polymers have been emerging as an effective way to increase efficacy of drugs and reduce side-effects. In this study, the DOC-loaded mPEG–PCL nanoparticles (DOC-NPs) were prepared, and the antitumor effect, in vivo distribution and penetration of DOC-NPs were comprehensively investigated. Significant tumor growth suppression was achieved when the DOC-NPs was given only one time at the low dose 10 mg/kg of DOC.

Taxanes are among the most effective anticancer drugs in the current clinical application, including breast cancer, ovarian, small and non-small cell lung cancer, head, neck and prostate cancer.

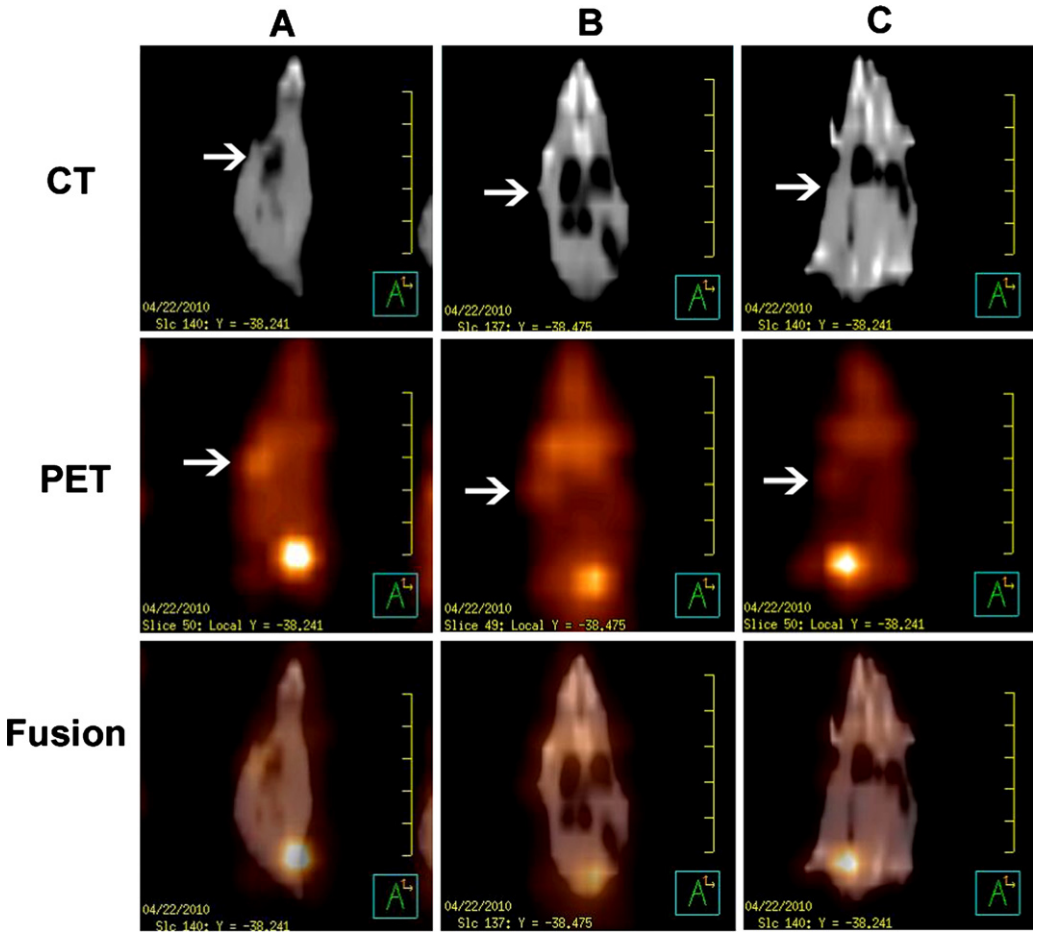

Fig. 8. PET-CT images of the tumor-bearing mice treated with saline (A), Taxotere® (B) and DOC-NPs (C) on the 7th day after treatment. The locations of tumors were indicated with white arrows.

Due to their poor aqueous solubility, they were currently formulated as a concentrated solution containing high amount of Tween 80 and ethanol, which might cause considerable toxicity (neutropenia, hypersensitivity, alopecia, water retention, dermatological reactions, etc.) (Baker et al., 2009; Bissery et al., 1995; Li et al., 2011). We prepared DOC-NPs with biodegradable mPEG–PCL copolymers because biodegradable nanoparticles had been highlighted as preferable intravenously injected targeted drug delivery systems to improve anticancer efficacy and decrease side effects in recent years.

The prepared DOC-NPs possessed high drug loading content and encapsulation efficiency with an appropriate size. DOC was released in a sustained manner from the polymeric nanoparticles with an initial burst. Such DOC release profile was ascribed to the following reasons: some encapsulated DOC was just on the surface of the nanoparticles (Chen et al., 2008), resulting in DOC quick diffusion from the nanoparticles to the medium. As a diffusion process, the in vitro drug release from nanoparticles was negatively influenced by drug loading content (drug density) in the nanoparticles (Chen et al., 2008; Zhu et al., 2010). Therefore, the in vitro DOC release was rapid in the beginning time, and became slow later because of a lower drug payload. In most previous studies, the drug release from nanoparticles was mainly conducted in PBS solution. As an intravenous injection, the performance in plasma is more important than that in PBS (Feng et al., 2011). In vitro cytotoxicity indicated that DOC still kept its pharmacological activity after it was released from the nanoparticles. These results were consistent with other similar reports by Kearns et al. (1995). They confirmed that the low-sustained concentration of Taxanes could more effectively kill tumor cells than high concentration of Taxanes with short exposure time. Therefore, the slow dissociation of DOC from polymeric nanoparticles might exhibit a more sustained release of the drugs in tumor sites and cause high tumor growth inhibition.

We evaluated the antitumor superiority of DOC-NPs over Taxotere® on subcutaneous inoculated H22 tumor bearing mice. This tumor model was selected because hepatocellular carcinoma was the third most common cause of cancer deaths and more than 60% of patients hardly received curative therapy due to the late clinical stage (Zhou et al., 2011; Thomas and Zhu, 2005; Edeline et al., 2009). The tumors growth in the Taxotere® treated group (10 mg/kg eq.) was as rapid as that of mice in the control group. There are several reasons why the Taxotere® did not inhibit the tumors growth. Firstly, H22 transplanted hepatic carcinoma is growing-fast and difficult to treat if the antitumor agents are not efficiently delivered to tumors. In our in vivo study, we "made" Taxotere® useless intentionally. It was reported the maximum tolerated dose of DOC for mice is about 20–50 mg/kg (Liu et al., 2008b). As you see, we chose Taxotere® at 10 mg/kg for one time, a dose which did not inhibit the tumor growth prominently, thus the effectiveness of the nanoparticles would be highlighted. Secondly, although, Taxotere® has been approved by FDA for the treatment of cancer, such as gastric cancer, colorectal cancer, and lung cancer, single Taxotere® for hepatic cancers treatment is disappointing. Many clinical studies have reported that singe docetaxel (Taxotere®) could not significantly suppress the hepatic carcinoma growth (Thomas and Zhu, 2005; He et al., 2010). Lastly but not leastly, the multidrug tumor resistance of systemic chemotherapy was frequently observed because of P-glycoprotein overexpression (Fardel et al., 1994; Payen et al., 1999; Kankesan et al., 2003). Unlike small molecular agents, the agents encapsulated in nanoparticles are usually internalized inside the cells by endocytosis pathways, reversing multidrug resistance (MDR) via inhibited P-glycoprotein (Pgp) function and Pgp ATPase activity (Xiao et al., 2011; Zhang et al., 2011; Gao et al., 2011; Riganti et al., 2011). The particle cellular uptake studies demonstrated sufficient interaction and internalization of mPEG–PCL nanoparticles with cancer cells. Thus, DOC could reach a high intracellular concentration with the nanoparticles formulation. This result was important for docetaxel to exert antineoplastic activity by binding to cytoplasmic microtubules.

On the contrary, a significant reduction of tumor growth was observed in the tumor-bearing mice treated with DOC-NPs. The result of PET/CT demonstrated the higher antitumor efficacy of DOC-NPs than free DOC formulation from the tumor metabolic activity standpoint. The increased cytotoxic effect of DOC-NPs could be reasonably explained with high DOC accumulation in tumors and uptake into the cells, mediated by NPs. In vivo NIRF imaging demonstrated that mPEG–PCL nanoparticles could not only target and deliver drugs to tumor (fluorescent signals of tumors from NIR-797 labeled nanoparticles began to appear 4 h post i.v. injection), but also eliminated from other normal tissues, which potentially decreased side effects. Tumor vasculatures, rather than those in normal tissues, have gaps as large as 10–1000 nm between adjacent endothelial cells (Petros and DeSimone, 2010; Ruoslahti et al., 2010). The permeable vasculatures coupled with impaired lymphatic system induce the EPR effect, which allows nanoparticles to extravasate through these gaps into extravascular spaces and accumulate inside tumor tissues. It was reported nanoparticles had a tendency to undergo reticuloendothelial system (RES) uptake, especially in the liver and spleen. The modification of PEG on the particles' surface creates a stealth function to avoid the uptake by other organs and extends the blood circulation (Hu et al., 2007; Karakoti et al., 2011; Jokerst et al., 2011). The nanoparticles with small size (<100 nm) could targetedly deliver anticancer drugs to tumor tissues through their inherent nanosize, the PEGylation, and the unique properties of the tumor microenvironment. The prepared mPEG–PCL nanoparticles might be a good candidate as an extended-time circulation drug delivery system.

The improved antitumor effect of DOC could also be attributed to an enhanced DOC penetration into the cells. The in vivo penetration studies of FITC-labeled nanoparticles suggested that a number of nanoparticles passively extravasated to tumors from leaky vessels by EPR effect after entering the blood. Then the FITC-labeled micelles distributed through interstitial space of the tumors, penetrated into the tumor zones. Our cellular uptake studies showed intact polymeric nanoparticles together with drugs were taken into cells, which was inconsistent with other reports. Therefore, incorporated docetaxel could also be delivered to tumor interior using nanoparticles as a carrier, followed by an increase antitumor activity. However, it was worth to note that the DOC-NPs could improve therapeutic effects in tumor-bearing mice rather than completely eradiate the tumors. The immunofluorescent study indicated that copolymeric nanoparticles with the size about 70 nm were not able to effectively permeate the tumor deeply and mainly affect the cells near or around the vasculature after entering the tumors. As a result, the tumors would be refractory after the treatment. Yuan et al. also found that liposomes formed perivascular clusters after leaking through the tumor vessels and they were not able to move significantly in tumor interstitial space (<20 μm in diameter away from the tumor vessels) (Yuan et al., 1994). Recent studies reported that administration of a transforming growth factor (TGF)-β inhibitor (TGF-β-1) or tumor penetrating peptide (iRGD) could enhance accumulation and antitumor activity of micellar nanomedicines (Teesalu et al., 2009; Skinner, 2010; Sugahara et al., 2010; Zhu et al., 2011; Cabral et al., 2011). The deep tumor accumulation of DOC-NPs in tumor tissues might pledge the antitumor efficacy. Therefore, we should take into account to further improve intratumoral penetration in the future study.

In terms of practical applications of targeting treatment, one of the key factors is to find suitable materials for loading the

anticancer drugs. An ideal material should be nontoxic, biodegradable, biocompatible with long circulating time. Herein, we used PEG-PCL copolymer as the drug carrier, because it has been approved by FDA to be used clinically. Even if a direct pharmakinetic study was not performed in the present study, these findings suggested that the high antitumor effect of DOC loaded into mPEG–PCL nanoparticles is mainly due to combinational effects of high cellular uptake efficiency, passive targeting ability induced by EPR effect and penetration improvement profile.

5. Conclusions

In this paper, DOC-loaded mPEG–PCL nanoparticles with high drug encapsulation and antitumor efficacy were successfully prepared by a modified nano-precipitation method. In vitro cellular uptake studies revealed that mPEG–PCL nanoparticles had high cellular uptake efficiency. The in vivo NIRF imaging revealed the DOC-NPs had prominent passive tumor-targeting ability. The penetration studies demonstrated that the mPEG–PCL nanoparticles were able to penetrate the tumor tissues after their extravasation through the leaky vessels and distribute in a distance of about 50 μm away from the vessels at 24 h post injection. More importantly, DOC-loaded mPEG–PCL nanoparticles displayed significant superiority of the anticancer activity compared to Taxotere®. We believe that the high effectiveness and biocompatibility of this simultaneous delivery system provides a promising approach for cancer therapy.

Acknowledgements

This work has been supported by the National Natural Science Foundation of China (Nos. 81172281, 81071815, 81101751, 81001408) and International Cooperation Plan of Nanjing Science and Technology Bureau (No. 201001137) and Nanjing Medical Science and technique Development Foundation (Level 3).

References

Baker, J., Ajani, J., Scotte, F., Winther, D., Martin, M., Aapro, M.S., von Minckwitz, G., 2009. Docetaxel-related side effects and their management. Eur. J. Oncol. Nurs. 13, 49–59.

Bissery, M.C., Nohynek, G., Sanderink, G.J., Lavelle, F., 1995. Docetaxel (Taxotere®): a review of preclinical and clinical experience. Part I: Preclinical experience. Anticancer Drugs 6, pp. 339–355, 363–338.

Cabral, H., Matsumoto, Y., Mizuno, K., Chen, Q., Murakami, M., Kimura, M., Terada, Y., Kano, M.R., Miyazono, K., Uesaka, M., Nishiyama, N., Kataoka, K., 2011. Accumulation of sub-100 nm polymeric micelles in poorly permeable tumours depends on size. Nat. Nanotechnol. 6, 815–823.

Chen, H., Kim, S., Li, L., Wang, S., Park, K., Cheng, J.X., 2008. Release of hydrophobic molecules from polymer micelles into cell membranes revealed by Forster resonance energy transfer imaging. Proc. Natl. Acad. Sci. U.S.A. 105, 6596–6601.

Cho, H.J., Yoon, H.Y., Koo, H., Ko, S.H., Shim, J.S., Lee, J.H., Kim, K., Kwon, I.C., Kim, D.D., 2011. Self-assembled nanoparticles based on hyaluronic acid-ceramide (HA-CE) and Pluronic(R) for tumor-targeted delivery of docetaxel. Biomaterials 32, 7181–7190.

Du, L., Mei, X., Wang, C., Li, X., Zhang, F., Jin, Y., 2011. In vitro/in vivo studies of the biodegradable poly-(D,L-lactide-co-glycolide) microspheres of a novel luteinizing hormone-releasing hormone antagonist for prostate cancer treatment. Anticancer Drugs 22, 262–272.

Edeline, J., Raoul, J.L., Vauleon, E., Guillygomac'h, A., Boudjema, K., Boucher, E., 2009. Systemic chemotherapy for hepatocellular carcinoma in non-cirrhotic liver: a retrospective study. World J. Gastroenterol. 15, 713–716.

Fardel, O., Loyer, P., Lecureur, V., Glaise, D., Guillouzo, A., 1994. Constitutive expression of functional P-glycoprotein in rat hepatoma cells. Eur. J. Biochem. 219, 521–528.

Feng, L., Wu, H., Ma, P., Mumper, R.J., Benhabbour, S.R., 2011. Development and optimization of oil-filled lipid nanoparticles containing docetaxel conjugates designed to control the drug release rate in vitro and in vivo. Int. J. Nanomed. 6, 2545–2556.

Gao, J., Zhong, W., He, J., Li, H., Zhang, H., Zhou, G., Liu, B., Lu, Y., Zou, H., Kou, G., Zhang, D., Wang, H., Guo, Y., Zhong, Y., 2009. Tumor-targeted PE38KDEL delivery via PEGylated anti-HER2 immunoliposomes. Int. J. Pharm. 374, 145–152.

Gao, Y., Chen, Y., Ji, X., He, X., Yin, Q., Zhang, Z., Shi, J., Li, Y., 2011. Controlled intracellular release of doxorubicin in multidrug-resistant cancer cells by tuning the shell-pore sizes of mesoporous silica nanoparticles. ACS Nano 5, 9788–9798.

Gradishar, W.J., Tjulandin, S., Davidson, N., Shaw, H., Desai, N., Bhar, P., Hawkins, M., O'Shaughnessy, J., 2005. Phase III trial of nanoparticle albumin-bound paclitaxel compared with polyethylated castor oil-based paclitaxel in women with breast cancer. J. Clin. Oncol. 23, 7794–7803.

He, A.R., Soe, K., El Zouhairi, M., 2010. Current problems with systemic treatment of advanced hepatocellular cancer. Curr. Probl. Cancer 34, 131–149.

Hu, Y., Xie, J., Tong, Y.W., Wang, C.H., 2007. Effect of PEG conformation and particle size on the cellular uptake efficiency of nanoparticles with the HepG2 cells. J. Control. Release 118, 7–17.

Jokerst, J.V., Lobovkina, T., Zare, R.N., Gambhir, S.S., 2011. Nanoparticle PEGylation for imaging and therapy. Nanomedicine (London) 6, 715–728.

Kankesan, J., Yusuf, A., Laconi, E., Vanama, R., Bradley, G., Thiessen, J.J., Ling, V., Rao, P.M., Rajalakshmi, S., Sarma, D.S., 2003. Effect of PSC 833, an inhibitor of P-glycoprotein, on 1,2-dimethylhydrazine-induced liver carcinogenesis in rats. Carcinogenesis 24, 1977–1984.

Karakoti, A.S., Das, S., Thevuthasan, S., Seal, S., 2011. PEGylated inorganic nanoparticles. Angew. Chem. Int. Ed. Engl. 50, 1980–1994.

Kearns, C.M., Gianni, L., Egorin, M.J., 1995. Paclitaxel pharmacokinetics and pharmacodynamics. Semin. Oncol. 22, 16–23.

Li, R., Li, X., Xie, L., Ding, D., Hu, Y., Qian, X., Yu, L., Ding, Y., Jiang, X., Liu, B., 2009. Preparation and evaluation of PEG-PCL nanoparticles for local tetradrine delivery. Int. J. Pharm. 379, 158–166.

Liu, Q., Li, R.T., Qian, H.Q., Yang, M., Zhu, Z.S., Wu, W., Qian, X.P., Yu, L.X., Jiang, X.Q., Liu, B.R., 2012. Gelatinase-stimuli strategy enhances the tumor delivery and therapeutic efficacy of docetaxel-loaded poly(ethylene glycol)–poly(varepsilon-caprolactone) nanoparticles. Int. J. Nanomed. 7, 281–295.

Li, X., Du, L., Wang, C., Liu, Y., Mei, X., Jin, Y., 2011. Highly efficient and lowly toxic docetaxel nanoemulsions for intravenous injection to animals. Pharmazie 66, 479–483.

Liu, B., Yang, M., Li, X., Qian, X., Shen, Z., Ding, Y., Yu, L., 2008a. Enhanced efficiency of thermally targeted taxanes delivery in a human xenograft model of gastric cancer. J. Pharm. Sci. 97, 3170–3181.

Liu, Z., Chen, K., Davis, C., Sherlock, S., Cao, Q., Chen, X., Dai, H., 2008b. Drug delivery with carbon nanotubes for in vivo cancer treatment. Cancer Res. 68, 6652–6660.

Payen, L., Courtois, A., Vernhet, L., Guillouzo, A., Fardel, O., 1999. The multidrug resistance-associated protein (MRP) is over-expressed and functional in rat hepatoma cells. Int. J. Cancer 81, 479–485.

Petros, R.A., DeSimone, J.M., 2010. Strategies in the design of nanoparticles for therapeutic applications. Nat. Rev. Drug Discov. 9, 615–627.

Riganti, C., Voena, C., Kopecka, J., Corsetto, P.A., Montorfano, G., Enrico, E., Costamagna, C., Rizzo, A.M., Ghigo, D., Bosia, A., 2011. Liposome-encapsulated doxorubicin reverses drug resistance by inhibiting P-glycoprotein in human cancer cells. Mol. Pharm. 8, 683–700.

Ruoslahti, E., Bhatia, S.N., Sailor, M.J., 2010. Targeting of drugs and nanoparticles to tumors. J. Cell Biol. 188, 759–768.

Salzano, G., Marra, M., Porru, M., Zappavigna, S., Abbruzzese, A., La Rotonda, M.I., Leonetti, C., Caraglia, M., De Rosa, G., 2011. Self-assembly nanoparticles for the delivery of bisphosphonates into tumors. Int. J. Pharm. 403, 292–297.

Skinner, M., 2010. Therapy: drugs hitch a ride. Nat. Rev. Cancer 10, 384.

Sugahara, K.N., Teesalu, T., Karmali, P.P., Kotamraju, V.R., Agemy, L., Greenwald, D.R., Ruoslahti, E., 2010. Coadministration of a tumor-penetrating peptide enhances the efficacy of cancer drugs. Science 328, 1031–1035.

Teesalu, T., Sugahara, K.N., Kotamraju, V.R., Ruoslahti, E., 2009. C-end rule peptides mediate neuropilin-1-dependent cell, vascular, and tissue penetration. Proc. Natl. Acad. Sci. U.S.A. 106, 16157–16162.

Thomas, M.B., Zhu, A.X., 2005. Hepatocellular carcinoma: the need for progress. J. Clin. Oncol. 23, 2892–2899.

Wong, C., Stylianopoulos, T., Cui, J., Martin, J., Chauhan, V.P., Jiang, W., Popovic, Z., Jain, R.K., Bawendi, M.G., Fukumura, D., 2011. Multistage nanoparticle delivery system for deep penetration into tumor tissue. Proc. Natl. Acad. Sci. U.S.A. 108, 2426–2431.

Wu, W., Li, R., Bian, X., Zhu, Z., Ding, D., Li, X., Jia, Z., Jiang, X., Hu, Y., 2009. Covalently combining carbon nanotubes with anticancer agent: preparation and antitumor activity. ACS Nano 3, 2740–2750.

Xiao, L., Xiong, X., Sun, X., Zhu, Y., Yang, H., Chen, H., Gan, L., Xu, H., Yang, X., 2011. Role of cellular uptake in the reversal of multidrug resistance by PEG-b-PLA polymeric micelles. Biomaterials 32, 5148–5157.

Yan, Y.D., Kim, D.H., Sung, J.H., Yong, C.S., Choi, H.G., 2010. Enhanced oral bioavailability of docetaxel in rats by four consecutive days of pre-treatment with curcumin. Int. J. Pharm. 399, 116–120.

Yuan, F., Leunig, M., Huang, S.K., Berk, D.A., Papahadjopoulos, D., Jain, R.K., 1994. Microvascular permeability and interstitial penetration of sterically stabilized (stealth) liposomes in a human tumor xenograft. Cancer Res. 54, 3352–3356.

Zhang, P., Ling, G., Sun, J., Zhang, T., Yuan, Y., Sun, Y., Wang, Z., He, Z., 2011. Multifunctional nanoassemblies for vincristine sulfate delivery to overcome multidrug resistance by escaping P-glycoprotein mediated efflux. Biomaterials 32, 5524–5533.

Zhou, J., Yu, L., Gao, X., Hu, J., Wang, J., Dai, Z., Wang, J.F., Zhang, Z., Lu, S., Huang, X., Wang, Z., Qiu, S., Wang, X., Yang, G., Sun, H., Tang, Z., Wu, Y., Zhu, H., Fan, J., 2011.

Plasma MicroRNA panel to diagnose hepatitis B virus-related hepatocellular carcinoma. J. Clin. Oncol. 29, 4781–4788.
Zhu, A.X., 2010. Systemic treatment of hepatocellular carcinoma: dawn of a new era? Ann. Surg. Oncol. 17, 1247–1256.
Zhu, Z., Li, Y., Li, X., Li, R., Jia, Z., Liu, B., Guo, W., Wu, W., Jiang, X., 2010. Paclitaxel-loaded poly(N-vinylpyrrolidone)-b-poly(epsilon-caprolactone) nanoparticles: preparation and antitumor activity in vivo. J. Control. Release 142, 438–446.
Zhu, Z., Xie, C., Liu, Q., Zhen, X., Zheng, X., Wu, W., Li, R., Ding, Y., Jiang, X., Liu, B., 2011. The effect of hydrophilic chain length and iRGD on drug delivery from poly(epsilon-caprolactone)–poly(N-vinylpyrrolidone) nanoparticles. Biomaterials 32, 9525–9535.